Seismicity preceding volcanic eruptions: New experimental insights

Luigi Burlini* Institute of Geology, ETH, Leonhardstrasse 19 LEB, CH-8092 Zurich, Switzerland
Sergio Vinciguerra HP-HT Laboratory, Istituto Nazionale di Geofisica e Vulcanologia, 00143 Rome, Italy
Giulio Di Toro Dipartimento di Geologia, Paleontologia e Geofisica, Università di Padova, 35137 Padua, Italy, and Istituto di Geoscienze e Georisorse, Unità operativa di Padova, CNR, Padova, Italy
Giuseppe De Natale Istituto Nazionale di Geofisica e Vulcanologia-Osservatorio Vesuviano, 80124 Naples, Italy
Philip Meredith Department of Earth Sciences, University College London, Gower Street, London WC1E 6BT, UK
Jean-Pierre Burg Institute of Geology, ETH, Leonhardstrasse 19 LEB, CH-8092 Zurich, Switzerland

ABSTRACT

A variety of seismic signals representing different physical mechanisms precedes volcanic eruptions. The most meaningful signals are high- and low-frequency earthquakes and volcanic tremor that have tentatively been related to fracturing and magma transport in the volcanic edifice. We provide experimental support for this association by reproducing magma migration while recording seismic signals. Opening fractures emit high-frequency acoustic events, while the switch to low frequency and harmonic tremor accompanies the flow of the melt in the fractures. Discerning between these seismic signals in nature can significantly refine volcanic hazard evaluation.

Keywords: rock physics, volcanic risk, volcanic tremor, acoustic emissions, melts, eruption precursor, volcanic hazard mitigation, seismic signals, seismicity.

INTRODUCTION

In volcanic hazard evaluation, the classification of different types of seismic signals plays a key role and has been interpreted with caution. The shape and characteristics (both in time and frequency domains) of the seismograms are related to geologic processes like fracturing, fluid oscillation, and melt migration. In active volcanic areas, two types of seismic signals are identified, together with hybrid earthquakes: (1) high-frequency seismicity that becomes more frequent during preeruptive phases. These seismic events produce high-amplitude P and S waves and have frequencies ranging from 5 to 15 Hz. These events may be caused by sudden fracturing or slip on faults, and typically occur as swarms (McNutt, 1996, 2000; Chouet, 2003; Troise et al., 2003). (2) Low-frequency earthquakes (LP, i.e., long period earthquakes) and volcanic tremor are often recorded prior to volcanic eruptions. These events often have emergent P waves, weak or null S waves, and dominant frequencies between 0.1 and 3 Hz. Two kinds of source mechanisms are commonly hypothesized: shallow LP events are ascribed to resonance of fluid-filled cavities, whereas deeper events are ascribed to magma movement (Kumagai et al., 2002, 2005). The very low frequency events (VLP, i.e., very long period, to 10^{-2}–10^{-3} Hz; Kawakatsu et al., 2000; Chouet, 2003; Chouet et al., 2005) are attributed to fluid-pressurization processes such as formation and collapse of bubbles (Aki and Koyanagi, 1981; McNutt, 1996, 2000; Chouet, 1996). Volcanic tremor is a quasi-continuous to continuous low-frequency signal that probably takes place from essentially the same mechanism as LP events, when the signal becomes continuous (Aki and Koyanagi, 1981; Julian, 1994; Ohminato et al., 1998). Volcanic tremor persists from minutes to days or longer. The important difference between volcano-tectonic events and LP tremor is that only the stressed rock is involved in the first class of signals, whereas LP and tremor involve oscillations of rock-fluid systems where fluids may be of geothermal or magmatic origin. Low-frequency earthquakes, VLP, and tremor are considered the best indicators of impending eruptions.

In order to consolidate the interpretation linking each type of seismic signal to any specific geologic process, we assembled an experimental setup simulating geologically relevant conditions in which a molten layer could intrude a bounding rock; acoustic emissions (AE) equivalent to seismic signals at laboratory scale were recorded during experiments. The seismic properties of the assembly during the experiments were also measured using the pulse transmission technique (Birch, 1960). Results bring a direct connection between high-frequency seismicity and crack formation and propagation, and between low-frequency seismicity and melt flow in open fractures.

Rock fracture and earthquake rupture are processes obeying similar statistics for source dimensions over more than eight orders of magnitude (Hanks, 1992; Zang et al., 1998). The Gutenberg-Richter relationship between frequency and magnitude of earthquakes also applies to experimental rock failure (Meredith et al., 1990; Sammonds et al., 1992). Moreover, AEs as well as earthquakes abide by power laws in time (Ponomarev et al., 1997; Feng and Seto, 1999) and spatial (Ponomarev et al., 1997; Lei et al., 2004) distribution of events. Thus, the main goals of AE studies so far have been (1) to characterize individual AE events in terms of their frequency content, amplitudes, and durations so that they can be related to the micromechanisms that produce them; (2) to analyze the statistics of recorded events to gain insights into the deformation processes and their rates; and (3) to locate the source of AE events in three dimensions to ascertain if the deformation is distributed or localized (Lockner et al., 1991).

Previous studies were carried out at room temperature and under low confinement pressure. Under these conditions, AE signals have high frequencies and represent either tensile events due to the opening of cracks or shear events due to the propagation and slip along cracks (Zang et al., 1998). The lack of high temperature and high confinement rupture experiments, simulating seismic signals under volcanic conditions, prevented a rigorous inductive-deductive association of seismic features with magma intrusion. This study takes advantage of rheological studies of partially molten mantle rocks to characterize experimentally the evolution of seismic signals during magma migration at simulated volcanic stress conditions, both recording AE generated within the sample and measuring seismic velocities.

METHODS AND RESULTS

Laboratory experiments were carried out in an internally heated gas rig (Paterson, 1970) (Paterson apparatus, Figs. 1A, 1C) at a confining pressure of 300 MPa and to a temperature of 1200 °C. The sample consisted of a 3-mm-thick disk of mid-oceanic-ridge basalt (MORB) glass sandwiched between two cylinders of olivine aggregates (Fig. 1B). The olivine cylinders were made with oven-dried San Carlos olivine powders (<50 μm grain size), which were cold pressed into Ni cans (to buffer the oxygen fugacity near the Ni-NiO buffer) and subsequently hot isostatic pressed at 1200 °C and 300 MPa for as long as 6 h in the Paterson apparatus. The synthetic olivine-aggregate samples, after jacket removal, were prepared in cylinders of ~10 mm length and 13 mm diameter. The glass cylinder was made from MORB powders (<15 μm grain size), which were cold pressed into Ni cans and

*E-mail: burlini@erdw.ethz.ch

© 2007 Geological Society of America. For permission to copy, contact Copyright Permissions, GSA, or editing@geosociety.org.

subsequently hot isostatic pressed at 1200 °C and 300 MPa for as long as 6 h in the Paterson apparatus. At these conditions the MORB was molten. After quenching to room temperature, melt solidified into a homogeneous glass and was cut into 3-mm-thick disks.

We recorded several seismograms with the pulse transmission technique while hot isostatic pressing the MORB powder in order to monitor the P-wave velocity, V_p, variation with temperature up to melting. These seismograms also show a decrease in amplitude of the seismic waves with increasing temperature (Fig. 2A). The dependence of wave amplitude with temperature suggests variations in the seismic properties of the MORB layer during the experiments described in the following, which were conducted within the same temperature range (20–1200 °C).

The olivine-MORB-glass-olivine assembly was jacketed in an iron tube and introduced in the rig with the cylinder axis being vertical. The experiment consisted of a heating phase from room temperature to 1200 °C at a rate of ~20 °C min^{-1} followed by a stationary phase where the temperature was kept at 1200 °C for ~70 min (Fig. 2B). AE output was monitored continuously throughout the experiment. Sporadic AE activity, characterized by relatively high frequency and energy, was recorded during heating (Fig. 3A). The most likely cause of this activity is thermal cracking and dilation of grain boundaries caused by the anisotropic thermal expansion of olivine crystals; thermal cracking and opening of grain boundaries increased sample porosity. An alternative source of high-frequency AE is slipping induced by the differential thermal expansion along the olivine-rod piston interfaces and along the iron jacket–sample interfaces. At ~640 °C (~20 min after the start of heating), ~40 AEs were recorded, characterized by low amplitude, short duration, and low energy (see GSA Data Repository Fig. DR1[1]). This temperature corresponds to the glass transition in the MORB glass (Giordano and Dingwell, 2003). After the onset of melting, a few high-frequency AEs were followed by a lower-frequency, long-lasting event of smaller and constant amplitude (Fig. 3C). The first part of this type of AE signal is characterized by short duration and a broad frequency spectrum, like the AE signals generated during thermal cracking. The second, long part of the AE signals is similar to the low-frequency seismicity (Fig. 3D).

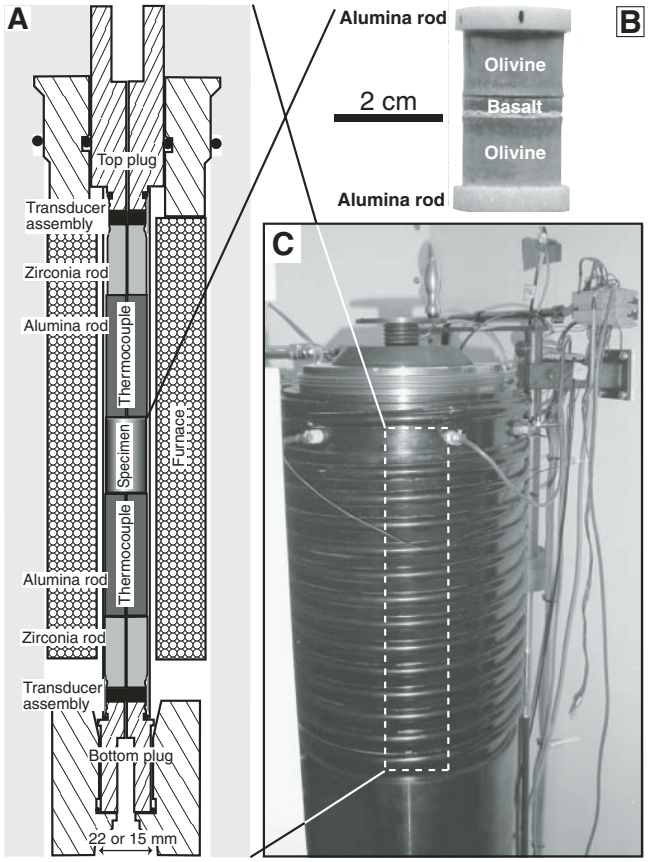


Figure 1. Experimental setup. A: Sketch depicting assembly inside vessel and furnace. Piezo elements are subjected to confining pressure but are away from hot zone. To maximize shape of thermal profile, both zirconia and alumina buffer rods were used; these two materials have very similar acoustic impedance. B: Sample assembly, composed of mid-ocean ridge basalt glass between synthetic olivine aggregate. Full alumina disks at top and bottom isolate sample. C: External view of Paterson rig apparatus, with electrical feed through for furnace and thermocouples. Black coil is pipe for cooling system.

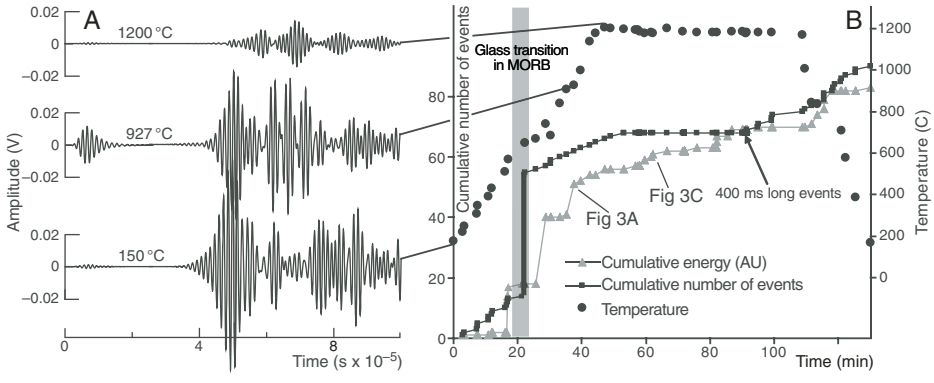


Figure 2. Experimental data. A: Seismograms recorded during P-wave velocity, V_p, measurements at three different temperatures on sample of pure mid-ocean ridge basalt (MORB) glass. Abscissa gives recorded arrival time in seconds, uncorrected for column delay. Velocity decreases as time increases, because length variations of assembly are minimal (few tens of microns). Note decrease of V_p and dramatic decrease of amplitude due to attenuation through melt between 927 °C and 1200 °C. B: Conduction of experiment of olivine and mid-ocean ridge basalt (MORB) with time. Line with full squares is cumulative curve of total number of acoustic emissions (AE), after filtering for noise events. Each square represents AE. At 20 min several AEs were recorded at glass transition of MORB glass. Very long lasting event of ~400 ms (Fig. DR2; see footnote 1) occurred at 91 min. Threshold was set to 45 dB at beginning, then at 46 dB after reaching 194 °C, 47 dB after reaching 609 °C, and at 48 dB at high temperature. (Figure 3A and Figure 3C are AE events shown in Fig. 3.) Line with triangles indicates cumulative energy in arbitrary units. Each triangle represents one event. Note that most of energy was recorded during heating. At high temperature, events were characterized by very low energy. Energy of events increased again during cooling.

[1]GSA Data Repository item 2007042, Figures DR1 (acoustic emission of the glass transition) and DR2 (acoustic emission during the intrusion of melt between jacket and sample), is available online at www.geosociety.org/pubs/ft2007.htm, or on request from editing@geosociety.org or Documents Secretary, GSA, P.O. Box 9140, Boulder, CO 80301, USA.

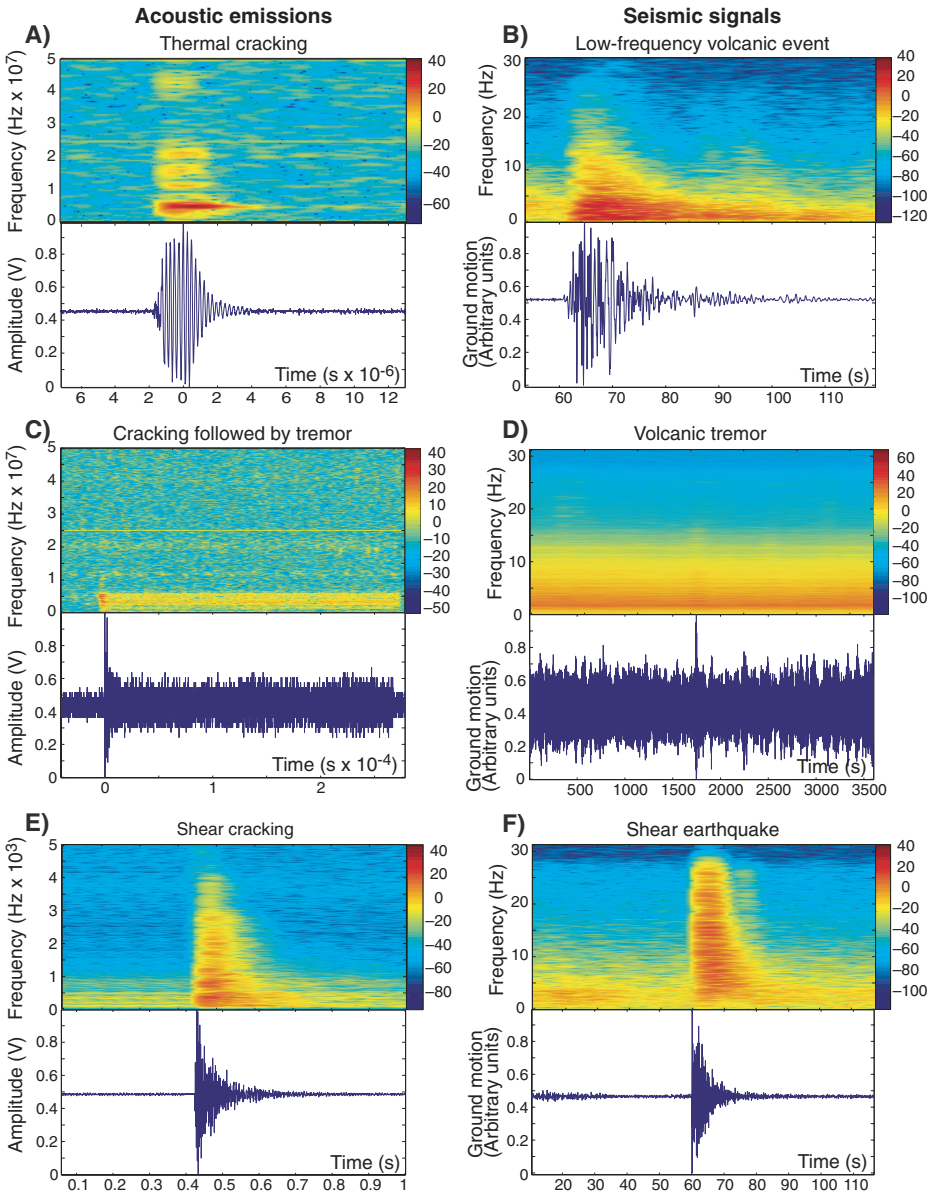


Figure 3. Normalized spectrogram (top) and seismogram (bottom) of (A) acoustic emission (AE) produced by thermal cracking; (B) Mount Etna low-frequency volcanic event, 2002–11–12 23:00; (C) AE of thermal cracking followed by tremor; (D) volcanic tremor at Mount Etna, 2002–04–11 10:22:21; (E) AE produced from shear cracking of ~10-mm-long fracture in basalt from Mount Etna (courtesy of S. Stanchits, GeoForschungsZentrum Potsdam), whereas AEs in A and C were emitted from ~100-µm-long fractures; (F) volcano-tectonic earthquake at Mount Etna, 2002–03–11 10:20:59. As frequency of AE decreases with increasing fracture size, AEs related to melt migration (C) have lower frequency than AEs produced by thermal cracking (A). Note similarities of natural events with microcracking and with tremor from experimental melt migration. Natural earthquakes are courtesy of G. Saccorotti (Istituto Nazionale di Geofisica e Vulcanologia, Naples).

After removal of the sample jacket, scanning electron microscope imaging of sections cut perpendicular to the layered assembly showed that melt from the basalt layer had migrated into the olivine layers through cracks across the top and bottom layers (Figs. 4B–4D). We speculate that the driving force for melt intrusion is given by the surface energy differences of the MORB-olivine interfaces, since the hydrostatic pressure is the same everywhere.

The monitoring of AEs and the subsequent microstructural analysis indicate that magma migration into cracks generates relatively low frequency seismic signals, which have the same qualitative waveforms as the natural seismograms related to magma intrusion.

DISCUSSION AND CONCLUSIONS

The fundamental similarity of the physical processes involved in generating low-frequency seismic signals in volcanoes and in laboratory experiments is established by comparing the spectral character and frequency scaling (Fig. 3).

1. AEs from thermal cracking during sample heating (Fig. 3A) have a markedly monochromatic spectrum, like volcanic low-frequency earthquakes (Fig. 3B).

2. The long-lasting tremor directly related to experimental melt migration (Fig. 3C) mimics recorded volcanic tremor (Fig. 3D).

3. Spectrograms of acoustic emission generated by shear failure (Fig. 3E) are almost identical to those of volcano-tectonic earthquakes (Fig. 3F).

Frequency scaling offers the strongest argument to assess equivalence of the physical processes between laboratory experiments and natural volcanic seismic signals. Experimental low-frequency events and tremor have frequencies of ~5 MHz for intrusion lengths between a few tens and 200 µm. In nature, volcanic low-frequency earthquakes with dominant frequencies of ~0–5 Hz are associated with fracture lengths of hundreds to 1000 m (McNutt, 2000). Considering that dominant frequencies of earthquakes scale inversely with source dimension (Aki and Richards, 1980), one may write $d_1 \times f_1 = d_2 \times f_2$, where d_1, d_2, f_1, and f_2 are dimension and frequency of laboratory (1) and nature (2). Comparing our laboratory data with typical frequency (1–2 Hz) and size (1 km) of low-frequency earthquakes, we obtain $d_2/d_1 = 5 \times 10^6$ and $f_1/f_2 = 2.5–5 \times 10^6$, indicating excellent agreement between laboratory information and natural cases.

The rapid amplitude decay of the laboratory-generated signal indicates that the waveforms are not significantly affected by further wave reflections inside the column and sample assembly (cf. Figs. 3A and 3B). Therefore, long-lasting events in laboratory are necessarily associated with long-lasting phenomena (cf. the traces of Figs. 3C and 3D).

These results provide a direct relationship between seismic behavior of rocks and seismic signal generation during magma injection and flow. In particular, melting is accompanied by a considerable reduction of wave velocities and increasing attenuation of the signal (Fig. 2B).

Magma intrusion is marked by a sequence of seismic signals occurring generally in dense swarms of very small events. In nature, high-frequency earthquakes are followed by low-frequency earthquakes that progressively merge in continuous tremor. These laboratory experiments provide evidence for understanding and discriminating the pattern of preeruptive seismicity at volcanoes. They validate on

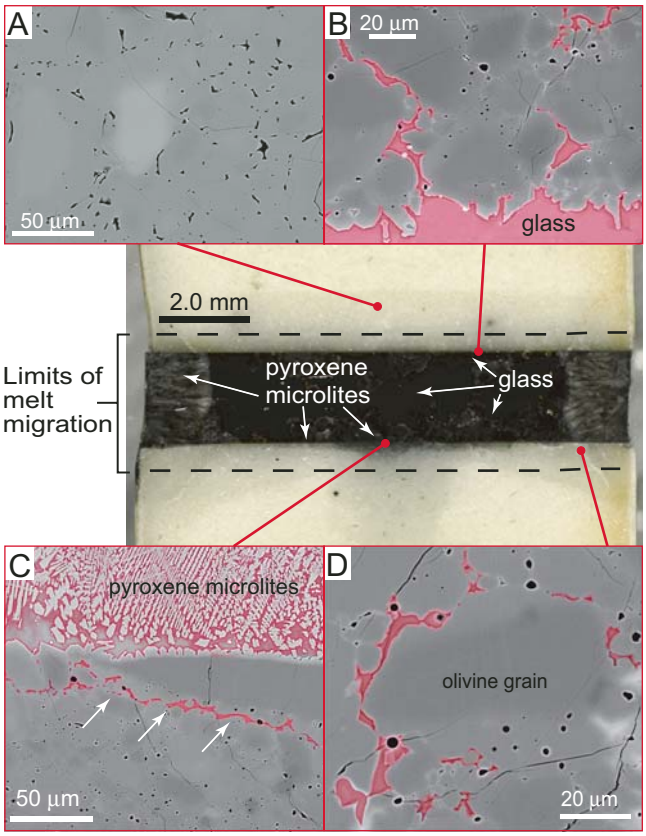


Figure 4. Backscattered scanning electron (BSE) microscope images of sandwich sample. Melt (glass) has been highlighted in pink in four BSE images. Black mid-ocean ridge basalt (MORB) layer in background figure consists of homogeneous glass and microlites of pyroxene. A: Melt is absent at 1000 µm from olivine-MORB interface. B: Melt intrusions are oriented at 95° and 65° from upper olivine–MORB interface. C: Melt intrusion oriented at 15° from lower MORB–olivine contact (white arrows). D: Melt intrudes fractures, grain boundary edge channels, and triple-point junctions at ~90 µm from olivine-MORB interface.

a physical basis the common assumption that low-frequency events and tremor indicate shallow magma intrusion that eventually leads to eruption. This experimental evidence improves the recognition of preeruptive seismic patterns and encourages new experimental analyses to better understand the details of low-frequency seismic emission during magma intrusion episodes, such as the intrusion in colder country rocks. Such results should allow a much higher reliability of eruption forecasts and thus have a strong impact on hazard mitigation.

ACKNOWLEDGMENTS

We thank A. Zappone for constructive discussions and suggestions, R. Hofmann and R. Prelicz for helping in the lab, and S. Stanchits and G. Dresen (GeoForschungsZentrum Potsdam) for providing the acoustic emissions from shear cracks and for fruitful discussions. The tests were conducted in the Experimental Deformation Laboratory at the Swiss Federal Institute of Technology (ETH) Zurich. This research was supported by Swiss National Science Foundation R'Equip project 2160-053289.98 and ETH Project 02150/41-2704.5 (Switzerland), Ministero dell'Università e della Ricerca (Italy), Progetto di Ateneo 2003 Università di Padova (Italy), and EU-Volcalert.

REFERENCES CITED

Aki, K., and Koyanagi, R., 1981, Deep volcanic tremor and magma ascent mechanism under Kilauea, Hawaii: Journal of Geophysical Research, v. 86, p. 7095–7109.

Aki, K., and Richards, P.G., 1980, Quantitative seismology: Theory and methods: San Francisco, California, Freeman & Co., 932 p.

Birch, F., 1960, The velocity of compressional waves in rocks up to 10 Kilobars: Part I: Journal of Geophysical Research, v. 65, p. 1083–1102.

Chouet, B., 1996, Long-period volcano seismicity: Its source and use in eruption forecasting: Nature, v. 380, p. 309–316, doi: 10.1038/380309a0.

Chouet, B., 2003, Volcanoes seismology: Pure and Applied Geophysics, v. 160, p. 739–788, doi: 10.1007/PL00012556.

Chouet, B., Dawson, P., and Arciniega-Ceballos, A., 2005, Source mechanism of Vulcanian degassing at Popocatepetl Volcano, Mexico, determined from waveform inversions of very long period signals: Journal of Geophysical Research, v. 110, no. B7, p. B07301, doi: 10.1029/2004JB003524.

Feng, X.T., and Seto, M., 1999, Fractal structure of the time distribution of microfracturing in rocks: Geophysical Journal International, v. 136, p. 275–285, doi: 10.1046/j.1365–246X.1999.0722x.x.

Giordano, D., and Dingwell, D.B., 2003,Viscosity of hydrous Etna basalt: Implications for Plinian-style basaltic eruptions: Bulletin of Volcanology, v. 65, p. 8–14, doi: 10.1007/s00445–002–0233–2

Hanks, T.C., 1992, Small earthquakes, tectonic forces: Science, v. 256, p. 1430–1432.

Julian, B.R., 1994, Volcanic tremor: Non linear excitation by fluid flow: Journal of Geophysical Research, v. 99, p. 11,859–11,877, doi: 10.1029/93JB03129.

Kawakatsu, H., Kaneshima, S., and Matsubayashi, H., 2000, Aso94: Aso seismic observation with broadband instruments: Journal of Volcanology and Geothermal Research, v. 101, p. 129–154, doi: 10.1016/S0377–0273(00)00166–9.

Kumagai, H., Chouet, B.A., and Nakano, M., 2002, Waveform inversion of oscillatory signatures in long-period events beneath volcanoes: Journal of Geophysical Research, v. 107, n. B11, 2301, doi: 10.1029/2001JB001704.

Kumagai, H., Chouet, B.A., and Dawson, P.B., 2005, Source process of a long-period event at Kilauea volcano, Hawaii: Geophysical Journal International, v. 161, p. 243–254, doi: 10.1111/j.1365–246X.2005.02502.x.

Lei, X., Masuda, K., Nishizawa, O., Jouniaux, L., Liu, L., Ma, W., Satoh, T., and Kusunose, K., 2004, Detailed analysis of acoustic emission activity during catastrophic fracture of faults in rock: Journal of Structural Geology, v. 26, p. 247–258, doi: 10.1016/S0191–8141(03)00095–6.

Lockner, D.A., Byerlee, J.D., Kuksenko, V., and Ponomarev, A., 1991, Observations of quasi-static fault growth and shear fracture energy in granite: Nature, v. 350, p. 39–42, doi: 10.1038/350039a0.

McNutt, S.R., 1996, Seismic monitoring and eruption forecasting of volcanoes; a review of the state-of-the-art and case histories, *in* Scarpa, R., and Tilling, R., eds., Monitoring and mitigation of volcanic of volcanoes: New York, Springer-Verlag, p. 99–146.

McNutt, S.R., 2000, Volcanic seismology, *in* Sigurdsson, H., et al., eds., Encyclopedia of volcanoes: San Diego, California, Academic Press, p. 1015–1033.

Meredith, P.G., Main, I.G., and Jones, C., 1990, Temporal variations in seismicity during quasi-static and dynamic rock failure: Tectonophysics, v. 175, p. 249–268, doi: 10.1016/0040–1951(90)90141-T.

Ohminato, T., Chouet, B.A., Dawson, P., and Kedar, S., 1998, Waveform inversion of very long period impulsive signals associated with magmatic injection beneath Kilauea volcano, Hawaii: Journal of Geophysical Research, v. 103, p. 23,839–23,862, doi: 10.1029/98JB01122.

Paterson, M.S., 1970, A high-pressure, high-temperature apparatus for rock deformation: International Journal of Rock Mechanics and Mining Sciences, v. 7, p. 517–526, doi: 10.1016/0148–9062(70)90004–5.

Ponomarev, A.V., Zavyalov, A.D., Smirnov, V.B., and Lockner, D.A., 1997, Physical modelling of the formation and evolution of seismically fault zones: Tectonophysics, v. 277, p. 57–81, doi: 10.1016/S0040–1951(97)00078–4.

Sammonds, P.R., Meredith, P.G., and Main, I.G., 1992, Role of pore fluids in the generation of seismic precursors to shear fracture: Nature, v. 359, p. 228–230, doi: 10.1038/359228a0.

Troise, C., Pingue, F., and De Natale, G., 2003, Coulomb stress changes at calderas: Modeling the seismicity of Campi Flegrei (southern Italy): Journal of Geophysical Research, v. 108, n. B11, 2292, doi: 10.1029/2002JB002006.

Zang, A., Wagner, F.C., Stanchits, S., Dresen, G., Andresen, R., and Haidekker, M.A., 1998, Source analysis of acoustic emissions in Aaue granite cores under symmetric and asymmetric compressive loads: Geophysical Journal International, v. 135, p. 1113–1130, doi: 10.1046/j.1365–246X.1998.00706.x.

Manuscript received 14 July 2006
Revised manuscript received 25 September 2006
Manuscript accepted 4 October 2006

Printed in USA